TRANSIENT MOTION OF SHIP DURING HARD GROUNDING

Jerzy Matusiak, Petri Varsta, Helsinki University of Technology, Ship Laboratory, P.O.Box 4100, FIN-02015 HUT, Finland

Phone: int+358+9+451 3480/ int+358+9+451 3500

Fax: int+358+9+451 4173

E-mail: Jerzy.Matusiak@Hut.Fi/Petri.Varsta@Hut.Fi

SUMMARY

A hard grounding of a ship is simulated. The results of computations are compared to the model test results. In the simulations transient motion of a rigid ship is evaluated. This motion is caused by a point force related to the local penetration of a hard obstacle into the ship hull. The location, magnitude and spatial orientation of this force depend upon the ship's instantaneous position and velocity in relation to the obstacle.
The dynamic response caused by hard grounding is solved in the time domain. The approach similar to the one presented earlier by Matusiak (2000, 2001) in the context of the intact ship stability problem is used. The total response of ship regarded as a rigid body having six degrees of freedom is evaluated in the time-domain. The non-linearities of the original model are preserved making it possible to consider large amplitude motions. A model unifying the radiation and manoeuvring hull forces in time-domain is presented. This model is based on the so-called convolution integral representation of the radiation forces with the modification allowing incorporating slow motion derivative values of the manoeuvring theory.

1. INTRODUCTION

There are several types of unwanted events during which ship's dynamic behaviour is of a transient type. Dynamic loss of stability in waves and response to wave impact are typical examples of such an event. Another problem is a powered hard grounding of ship considered in this paper.

2. MATHEMATICAL MODEL OF SHIP RIGID BODY MOTIONS

A ship is regarded as a rigid body possessing six degrees of freedom. Flooding is not taken into account.

2.1 MOTION KINEMATICS

Three co-ordinate systems are used for describing ship motion. These are presented in Figure 1. An inertial Cartesian co-ordinate system fixed to Earth is denoted by *XYZ*. *X*-axis points to the initial direction of ship velocity. The *X*-*Y* plane coincides with the still water level and *X*-axis is initially located in the centre-plane of ship. The origin *0* of this co-ordinate system is located at the vertical passing through the tip of the rock. *G* denotes the ship's centre of gravity, which is the origin of the Cartesian co-ordinate system *xyz* fixed with the ship with *x*-axis pointing towards bow. This co-ordinate system is called the body-fixed co-ordinate system. The so-called horizontal body axes co-ordinate system (Hamamoto &Kim, 1993) denoted as $\xi\eta\zeta$ moves also with the ship so that the axes ξ, η and ζ are parallel to the axes of the Earth-fixed co-ordinate system *XYZ*.

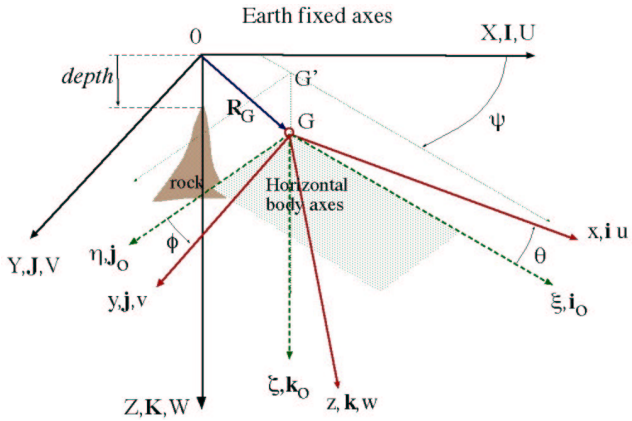

Figure: 1 Co-ordinate systems used to describe motion of a ship.

The instantaneous position of ship's center of gravity *G* is given by the following displacement components: surge ξ, sway η and heave ζ. These are the motion components of the center of gravity in the moving co-ordinate system $\xi\eta\zeta$. The velocity of the origin of ship is given as

$$\boldsymbol{U} = \dot{\boldsymbol{R}}_G = \dot{X}_G\boldsymbol{I} + \dot{Y}_G\boldsymbol{J} + \dot{Z}_G\boldsymbol{K} = u\boldsymbol{i} + v\boldsymbol{j} + w\boldsymbol{k} \quad , \quad (1)$$

where *u, v* and *w* are the projections of the velocities $\dot{X}_G, \dot{Y}_G$ and $\dot{Z}_G$ of the ship's centre of gravity in the Earth-fixed inertial co-ordinate system on the axes of the moving body-fixed system. The angular position of the ship is given by so-called modified Euler angles denoted in Fig. 1 as ψ, θ and ϕ. These angles bring a vehicle from the reference (initial) orientation to the actual orientation of the body-fixed co-ordinate system. The orientation of the body-fixed co-ordinate system varies in time. The following matrix relation (Clayton & Bishop, 1982; Fossen, 1994) gives the projection of the velocity expressed in body-fixed co-ordinate system on the Earth-fixed co-ordinates

$$\begin{Bmatrix} \dot{X}_G \\ \dot{Y}_G \\ \dot{Z}_G \end{Bmatrix} = \begin{bmatrix} \cos\psi\cos\theta & \cos\psi\sin\theta\sin\phi - \sin\psi\cos\phi & \cos\psi\sin\theta\cos\phi + \sin\psi\sin\phi \\ \sin\psi\cos\theta & \sin\psi\sin\theta\sin\phi + \cos\psi\cos\phi & \sin\psi\sin\theta\cos\phi - \cos\psi\sin\phi \\ -\sin\theta & \cos\theta\sin\phi & \cos\theta\cos\phi \end{bmatrix} \begin{Bmatrix} u \\ v \\ w \end{Bmatrix}. \quad (2)$$

Angular velocity Ω of the ship in the body fixed co-ordinate system is

$$\mathbf{\Omega} = P\mathbf{i} + Q\mathbf{j} + R\mathbf{k}\,. \quad (3)$$

The dependence of the derivatives of the Euler angles and angular velocity components of equation 3 is as follows (Clayton & Bishop, 1982)

$$\begin{Bmatrix} \dot{\phi} \\ \dot{\theta} \\ \dot{\psi} \end{Bmatrix} = \begin{bmatrix} 1 & \sin\phi\tan\theta & \cos\phi\tan\theta \\ 0 & \cos\phi & -\sin\phi \\ 0 & \sin\phi/\cos\theta & \cos\phi/\cos\theta \end{bmatrix} \begin{Bmatrix} P \\ Q \\ R \end{Bmatrix}. \quad (4)$$

2.2 EQUATIONS OF MOTION

Equations of motion are given by the set of six non-linear ordinary differential equations (Fossen, 1994)

$$\begin{aligned} X_g - \mathrm{m}g\sin\theta &= \mathrm{m}(\dot{u} + Qw - Rv) \\ Y_g + \mathrm{m}g\cos\theta\sin\phi &= \mathrm{m}(\dot{v} + Ru - Pw) \\ Z_g + \mathrm{m}g\cos\theta\cos\phi &= \mathrm{m}(\dot{w} + Pv - Qu) \end{aligned} \quad (5)$$

$$\begin{aligned} K_g &= I_x\dot{P} - I_{xy}\dot{Q} - I_{xz}\dot{R} + (I_zR - I_{zx}P - I_{zy}Q)Q \\ &\quad - (I_yQ - I_{yz}R - I_{yx}P)R \\ M_g &= -I_{yx}\dot{P} + I_y\dot{Q} - I_{yz}\dot{R} + (I_xP - I_{xy}Q - I_{xz}R)R \\ &\quad - (I_zR - I_{zx}P - I_{zy}Q)P \\ N_g &= -I_{zx}\dot{P} - I_{zy}\dot{Q} + I_z\dot{R} + (I_yQ - I_{yz}R - I_{yx}P)P \\ &\quad - (I_xP - I_{xy}Q - I_{xz}R)Q. \end{aligned}$$

In equations 5, X_g, Y_g, Z_g, K_g, M_g and N_g depict the components of global reaction force and moment vectors acting on the ship. These are given in the-body fixed co-ordinate system xyz. *m* and I_{ij} mean ship's mass and the components of the mass moment of inertia.

2.3 REACTION FORCES CONSIDERED IN THE MODEL

Reaction forces and moments considered in the model comprise the ship resistance, restoring, radiation, manoeuvring and forces and moments associated with grounding.

2.3 (a) Resistance

The resistance of ship in still water was evaluated using model scale tests. The resistance curve was fitted with cubic splines as a function of velocity component *u*. In the simulations, an instantaneous value of resistance is evaluated. Resistance contributes to X_g reaction force component only. The action of propeller is inactivated in order to simulate model test experiments. Rudder is fixed in the neutral position.

2.3 (b) Combined Model Of Manoeuvring Hull And Radiation Forces In the Time Domain

A linear model making use of the added mass and damping concept approximates radiation forces. These forces can be expressed as

$$\begin{aligned} X_{\mathrm{rad}} &= -a_{11}\dot{u} - a_{15}\dot{Q} - b_{15}Q \\ Y_{\mathrm{rad}} &= -a_{22}\dot{v} - b_{22}v - a_{24}\dot{P} - b_{24}P - a_{26}\dot{R} - b_{26}R \\ Z_{\mathrm{rad}} &= -a_{33}\dot{w} - b_{33}w - a_{35}\dot{Q} - b_{35}Q \\ K_{\mathrm{rad}} &= -a_{44}\dot{P} - b_{44}P - a_{46}\dot{R} - b_{46}R - a_{42}\dot{v} - b_{42}v \\ M_{\mathrm{rad}} &= -a_{55}\dot{Q} - b_{55}Q - a_{53}\dot{w} - b_{53}w - a_{51}\dot{u} \\ N_{\mathrm{rad}} &= -a_{66}\dot{R} - b_{66}R - a_{64}\dot{P} - b_{64}P - a_{62}\dot{v} - b_{62}v. \end{aligned} \quad (6)$$

In equations (6) a_{ij} and b_{ij} depict added masses and damping coefficients referred to the origin located in the centre of gravity (G in Fig. 1). These have frequency dependent values. They are evaluated by a standard linear seakeeping theory based computer program (Journee, 1992). Note that radiation forces are oriented in the body-fixed co-ordinate system.

Memory effect included using the retardation function concept

Time domain approach requires the so-called convolution integral representation of the radiation forces (Cummins, 1962). In this approach radiation forces vector $\mathbf{X}_{\mathrm{rad}}$ is represented by an expression:

$$\mathbf{X}_{rad}(t) = -\mathbf{a}_\infty\ddot{\mathbf{x}}(t) - \int_{-\infty}^{t}\mathbf{k}(t-\tau)\dot{\mathbf{x}}(\tau)d\tau\,, \quad (7)$$

where $\mathbf{a}_\infty$ is the matrix comprising the added masses coefficients for an infinite frequency and $\mathbf{x}$ is the response vector. Matrix function $\mathbf{k}$ is the so-called

retardation function, which takes into account the memory effect of the radiation forces. This function can be evaluated as

$$\mathbf{k}(t) = \frac{2}{\pi}\int_0^\infty \mathbf{b}(\omega)\cos(\omega t)d\omega\,, \qquad (8)$$

where **b** is the frequency dependent added damping matrix. In order to take into account the maneuvering hull forces four components of the **b** matrix are modified as follows. Terms of sway (Y_V), yaw (N_R) and their coupling terms (N_V and Y_R) of the linear hull forces model are subtracted from the corresponding elements of matrix **b**, i.e.

$$b'_{22}(\omega) = b_{22}(\omega) - Y_V$$

$$b'_{66}(\omega) = b_{66}(\omega) - N_R \qquad (9)$$

$$b'_{62}(\omega) = b_{62}(\omega) - N_V$$

$$b'_{26}(\omega) = b_{26}(\omega) - Y_R.$$

k*(t)* functions have to be evaluated only once before the simulation. The *Fast Fourier Transform* algorithm is used when evaluating discrete values of the retardation functions. Details of the algorithm were presented by Matusiak (2001).

2.3 (c) Restoring Forces And Moments

The non-linear three-dimensional model is used when evaluating the restoring forces and moments. The ship hull is discretized by a number of plane panels (see Fig. 2).

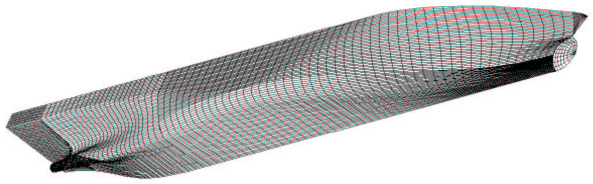

Figure 2: Bottom view of Ro-Ro ship.

The following quantities represent a single panel element: co-ordinates of a control point, normal vector and area. At each time step, the hydrostatic pressures over the immersed panels are evaluated and summed up into the restoring forces and moments.

2.3 (d) Contact Force Due To Grounding

A single force vector represents grounding. At each time step of the simulation, the minimum distance between the control points representing hull and rock tip is sought. This distance determines whether the contact occurs, it gives the panel number at which contact occurs and the penetration. Moreover, the direction of relative velocity between the panel and the rock tip is determined. If contact occurs and normal component of the relative velocity points inside hull, contact force is evaluated. Both the normal and the tangential component of the contact force are assumed to be simple functions of a penetration. The constitutive relation of the force and the penetration was obtained by conducting the intender tests of the material used in the model test experiments (Lax, 2001). In these tests the bottom of ship model was constructed of the fully plastic (inelastic foam) which when scaled to the ship's scale gave realistic values of the contact force as a function of the penetration.

3. MODEL TESTS

Model tests of two vessels (a tanker and a RoPax-ship) were conducted (Lax, 2001). The model scale was 45. A novel technique was developed in order to have a realistic modelling of contact force and ship dynamics. The ship bottoms were constructed of a soft inelastic urethane material. Tests were conducted with a model accelerated to a prescribed speed and let freely proceed for a couple of meters before impacting an underwater instrumented rigid obstacle of a conical form. Three components of contact force and motions of the model were measured in the tests. Model speed and location of initial contact were varied. Moreover, the penetration caused by intender in a model bottom was measured after the tests.

Apart conducting model tests, Lax has also done a quasi-static analysis of the hard grounding events. His conclusion was that disregarding dynamics yields a significant underestimation of a damage length.

4. RESULTS OF SIMULATION AND THEIR COMPARISON WITH THE MODEL TESTS

From many measured and simulated grounding events only one, most interesting is presented in the following for the sake of brevity. The vessel is a modern RoPax-ship of a length L_{pp} = 146 [m], draft T = 7.35 [m], breadth B = 25.35 [m], block coefficient C_B = 0.65 and volumetric displacement ∇ = 17630 [m^3].

Table 1: The natural periods of the RoPax- ship.

Motion component	Natural period [s]
Roll	16.8
Pitch	7.4
Heave	7.2

The initial speed of ship is 12 [kn]. A rigid obstacle of a conical form is located 5 [m] from the ship's centre plane to port. The distance of the tip of it to still water level is

6.885 [m]. The natural periods of the ship motions are as follows (Lax, 2001):
The bottom view of the investigated ship and the contact line due to grounding are shown in Fig. 3.

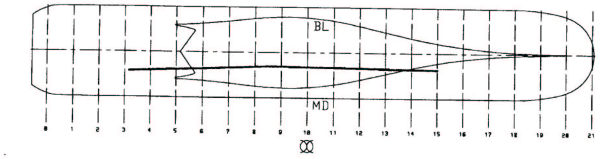

Figure 3: The bottom view of the investigated ship and the contact line due to grounding.

Both, the simulated and the measured in model tests forces during the grounding event are presented in Fig. 4-6.

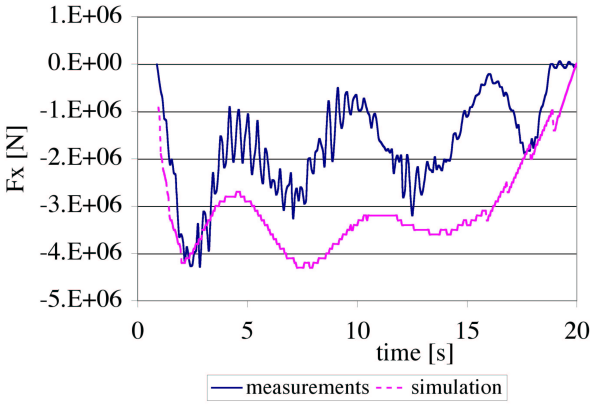

Figure 4: The longitudinal (x-component) of the force due to grounding.

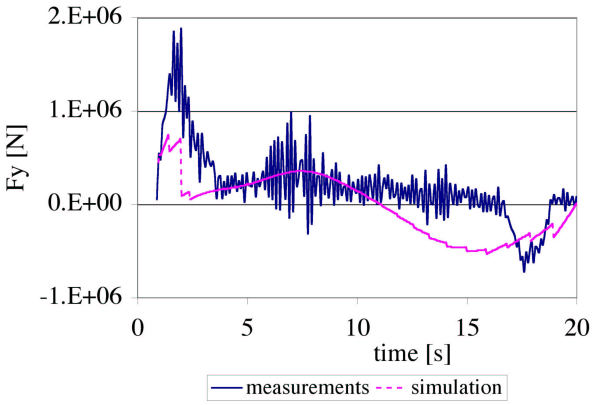

Figure 5: The transverse (y-component) of the force due to grounding.

Measured values are scaled to full-scale. A qualitative agreement of the results is noted. Main part of the force variation happens with the frequency close to the natural frequencies of the ship motions. This indicates that hard grounding is indeed associated with the dynamic ship responses. Also a higher frequency variation associated either with the dynamic response the force gauges or caused by model whipping is visible. This can be disregarded as a spurious one. The simulation reproduces well the maxima of the x- and z-components of the grounding force. The duration of the contact event is predicted accurately as well. The simulation overestimates local maxima of the grounding force following the first impact and underestimates the transverse component of the force.

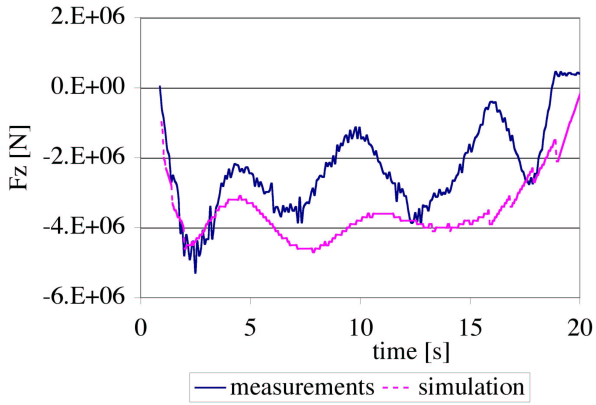

Figure 6: The vertical (z-component) of the force due to grounding.

The forward velocity of the ship as measured in model scale and as simulated is presented in Fig. 7. Two zones of a deceleration are visible. The first one, steeper one, is caused by the x-component of the grounding force (see Fig. 4). Somewhat overestimated simulated braking force causes faster deceleration of the ship at this stage. When the ship is free from the grounding contact, measured deceleration is faster than the simulated one because of a higher frictional resistance of the model.

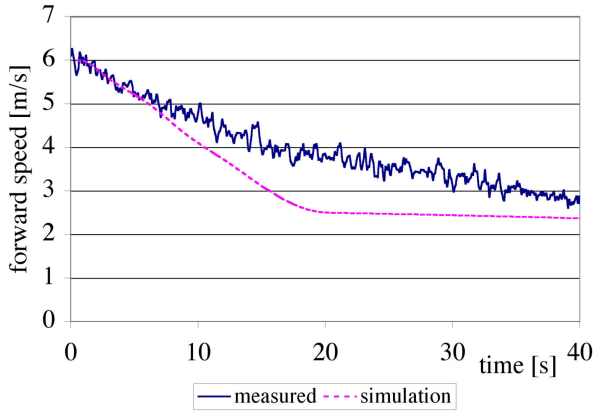

Figure 7: Measured and simulated forward velocity of model and ship.

Unfortunately, measurements of the ship model motions conducted during the grounding tests can be regarded as qualitative ones, only. The measuring system comprised of stiff wires connected to the potentiometers and angular velocities measuring device. In principle integrating the velocities yields the angular motions. Unfortunately, low value transient responses of yaw and pitch rates when integrated yield wrong results. The only motion component that was measured with a sufficient accuracy

is roll. Comparison of measured and simulated roll is shown in Fig. 8.

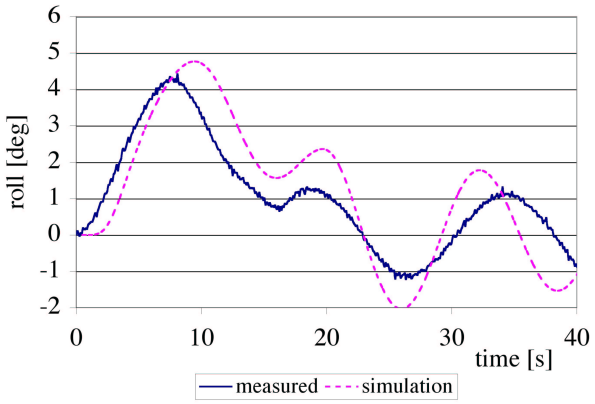

Figure 8: The roll due to the grounding as measured in model scale and as simulated.

A good agreement of the simulated and the measured roll is noted. The roll motion is caused mainly by the z-component of the grounding force acting at approximately quarter of ship's breadth off the centre plane at the port. Unfortunately validation of other motion components is not possible because of the above-mentioned problems encountered in the model tests. For these reasons only the simulated heave and pitch motion components are presented in Fig. 9.

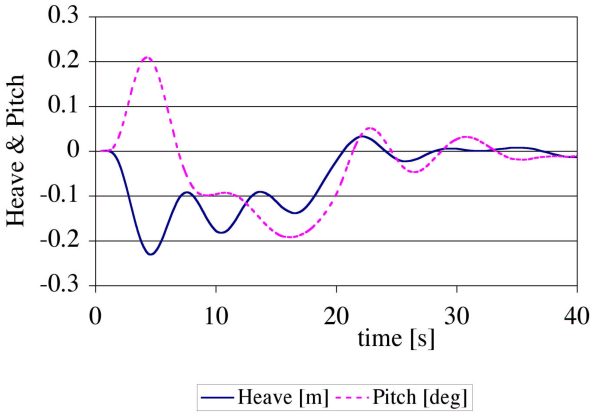

Figure 9: The simulated heave and pitch motion due to the grounding.

They show reasonable behaviour. Pitch and heave reach the maxima as a result of the first impact. The sign of pitch changes when the contact point moves from the bow aft-wards of the centre of gravity. Heave stays negative for the entire duration period of the grounding contact.
A simplified model of ship dynamics based on the constant added masses and damping coefficient was tried at an early stage of the method development. The results obtained with this model differed much from the ones presented above. Both the grounding force and the ship response were associated with the periods that were different from the ones obtained in model test experiments.

5. CONCLUSIONS

Both the model tests and the numerical simulations prove that during a hard powered, that is at speed, grounding ship's behaviour is governed by dynamics. There is a strong interaction between the ship motion and the causing it grounding force. As the response of ship is of a transient type, a special care has to be taken when modelling the radiation forces. A straightforward approach based on a constant added masses and damping coefficients is not appropriate.
A relatively simple relation between the grounding force and the penetration was used in order to simplify the numerical simulations and in order to get a realistic ship response both in the model tests and in the computations. Moreover, this simple relation makes it possible to validate the presented procedure. A separate project aimed at evaluating local strength of double bottom structures has been recently completed (Naar et al, 2002; Tabri, 2002). The results of this study may be incorporated into the presented method in the future. Other problems that can be considered too are the effect of transient flooding and the influence of shallow water on the ship dynamics during grounding.

6. ACKNOWLEDGEMENT

The authors express their sincere thanks to Dr. Juri Kajaste-Rudnitski for his assistance in development and implementation of the contact model used in the presented method. The financial support of the National Technology Agency, Kværner Masa-Yards and Aker Finnyards is greatly appreciated.

7. REFERENCES

Clayton B.R.& Bishop R.E.D, 1982. Mechanics of marine vehicles, ISBN 0 419 12110-2.
Cummins, W.E. 1962. The Impulse Response Function and Ship Motions,Schiffstechnik 9, Nr. 47 S101/109.
Fossen, T.,I. 1994. Guidance and control of ocean vehicles, J. Wiley&Sons, ISBN 0 471 94113 1.
Hamamoto, M. and Kim, Y.S. 1993 "A New Coordinate System and the Equations Describing Manoeuvring Motion of a Ship in Waves," J. Soc. Naval Arch., Vol 173.
Journee. J. M. 1992. Strip Theory Algorithms, report MEMT 24, Delft University of Technology, Ship Hydrodynamics Laboratory.
Lax, R. 2001. Ship model tests of hard grounding, Helsinki University of Technology, Report M- 260, (in Finnish).

Matusiak, J. 2000. Two-Stage Approach To Determination Of Non-Linear Motions Of Ship In Waves, 4th Osaka Colloquium on Seakeeping Performance of Ships, Osaka, Japan, 17-21st October, 2000

Matusiak, J. 2001. Importance Of Memory Effect For Capsizing Prediction, *5th International Workshop On Ship Stability*, University of Trieste 12. - 13. September 2001.

Naar, H., Kujala, P., Simonsen, B.C., Ludolphy, H., 2002. Comparison of the crashworthiness of various bottom and side structures. Marine Structures 15 (2002), Pp. 443-460.

Tabri, K. 2002. FE simulation of a double-bottom grounding on a conical rock. Helsinki University of Technology, Ship Laboratory, Espoo 2002, Report M-271.